Journal of the Nigerian Association of Mathematical Physics
Volume 60 **(April – June** *2021 Issue***), pp171 –182**

DESIGN AND IMPLEMENTATION OF A 40A, 12V SOLAR CHARGE CONTROLLER WITH PULSE WIDTH MODULATION

Omorogiuwa O.S. and Iyekekpolo E.N.

Department of Electrical/Electronic Engineering,
Faculty of Engineering, University of Benin, Benin City. Nigeria.

Abstract

This study is to design and construct a Charge Controller using Pulse Width Modulation (PWM), in which a lead-acid battery can be charged using a solar panel as the power source, and having a battery monitoring subsystem for full-charge cut-off protection.
The method adopted is through a feasibility study involving research of existing units of solar chargers that use the on/off technique of battery charging, followed by observation and testing to determine their efficiency and shortcomings. Based on the research, charge control using pulse width modulation was chosen as a good technique for battery charging due to several advantages. Major components used in designing such controllers include a variable resistor, a microcontroller (PIC16F88), an integrated circuit socket, electrolytic capacitors, a veroboard, circuit connectors (100A), diodes, a MOSFET (IRFP260N), heatsinks, etc.
A functionality test was carried out after the circuit was completed. During testing, a 32.3V-rated solar panel and a 12V, 100AH battery were connected to the completed charge controller circuit. The solar panel functioned as the power source of the circuit, and the battery as the circuit load. The system worked satisfactorily by charging the battery successfully. Results obtained indicated that the battery attained a good charge level after two (2) hours of charging through the circuit, this showing that the charge control system worked as it was designed to.

Keywords: AC (Alternating Current), DC (Direct Current), Charge Controllers, Microcontroller, MOSFET, MPPT, PMW, PV Solar Array

1.0 INTRODUCTION

The advent of electricity has been described as a revolutionary discovery that has been a major driving force in the advancement of contemporary civilization. Electricity is often called the lifeblood of contemporary life. Buttressing this appellation is the rise of increasingly helpful electric machines that power a wide range of appliances that are designed to make life as we know it comfortable or even possible. Electric power has now come to be solely depended on for nearly everything. Practically all modern home appliances are powered by electricity. Electricity and the devices powered by it have become so important that in most part of the world, comfort, work, and even life will be inconceivable. Thus, in many parts of the world, a lot of resources and invested into establishing sustainable sources of stable power supply to ensure the continued wellbeing of people.

Before the wide adoption of AC power, which was discovered by the late Nicola Tesla in the early 20th century, batteries were the main sources of power for electric appliances. Even in our current world, DC storage batteries are still used to power a wide range of electrical loads or appliances that are designed to have DC power inputs.

Corresponding Author**:** Omorogiuwa O.S., Email: sam@uniben.edu, Tel: +2348056127223, +2347061280886 (IEN)

Batteries play a very significant role in our day-to-day activities, they are applied in all sorts of machines ranging from those applied in the home (like cars, wristwatches, GSM phones), to those utilized for industrial purposed. Batteries are commonly classified under two types: primary and secondary batteries [1]. Primary cells (where a cell is a unit of a battery), are those batteries that cannot be recharged after use. They are designed to continuously supply current until the electrolyte is exhausted or the negative electrode is completely dissolved.

The secondary cells in contrast, can be recharged by passing the right type of current through them [2]. Charging battery cells is attained by passing DC of suitable ampere value in the opposite direction to the current that normally flows from the cell to a load, ensuring that the electrode surface is reformed and the electrolyte returns to its original state.

The commercial use of the lead-acid battery is over 100 years old. In 1859, Gaston Planté (French physicist) invented the Lead-acid battery, which is the oldest type of rechargeable battery [3].

Rechargeable batteries with their relatively affordable cost, are ideal for use in automobiles as they can provide the high inrush current required by automobile starter motors [4]. They are also used in vehicles used for lifting such as forklifts, in which their low energy-to-weight ratio may be considered a benefit since the battery can be used as a counterweight. Large collections of lead-acid cells are used as standby (or backup) power sources for telecommunications facilities, generating stations, and computer data centers [5]. They are also used to power the electric motors in diesel-electric (conventional) submarines and recently, as a source of DC power for inverter powered systems.

Lead-acid batteries and the alkaline batteries are the two major types of rechargeable battery in common use.

Despite their many advantages, storage batteries must be recharged once they are discharged, so that they do not lose their lifespan capacity, or in the case of lead-acid battery, suffer from sulfation. For optimal charging from renewable sources, a charge controller is used to charge recharge these batteries to ensure that the charging current is adequate.

A charge controller is a device that has been designed to recharge rechargeable batteries from renewable sources. They provide regulated DC power to recharge rechargeable batteries from renewable power sources. It could convert power from an AC source to DC of the suitable voltage to charge batteries or from another DC source that has an unsuitable voltage level. It should be noted that batteries are also very sensitive to long delays of no-recharge after they have been discharged.

The failure of the electric power utilities to supply constant power to the consumers has led the consumers to find alternative ways of power supply to recharge their batteries using generators and recently, solar panels.

The discovery of the photovoltaic effect of the sun's rays on certain elements gave birth to PV solar cell technology that could supply DC power which it generates from light rays. The advantage of this alternative source of power is that the sun’s rays are free and constitute an endless source of power. Also, solar panels have a useful life of about 25 years [6]. This altogether means a cheap and clean source of power over a long period of time.

Solar panels are commonly used for charging batteries in inverters or UPS. Its popularity is due to the growing use of inverters as an alternative source of power for domestic uses. The solar panel is an important source of energy for battery charging because of the epileptic nature of power supply in technologically underdeveloped countries.

This study was borne out of the need to design a portable, simple and effective charge controller device that can help vehicle and inverter owners easily charge their batteries conveniently and when needed.

The circuit design is illustrated in the block diagram in Figure 1.

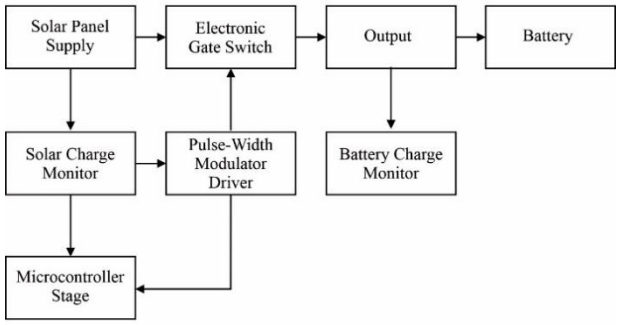

Figure 1. Block diagram of the Solar Charge Controller using Pulse Width Modulator

2.0 Design Methodology

This section presents the design analysis of the solar charge controller using a pulse width modulation technique. The control circuit system functional block is shown in Figure 2. The block diagram shows the functional stages of the charge controller and what they are made of and how they are interconnected. The design of the system would be presented in the following sections according to the block diagram representation.

The microcontroller monitors the solar power to the battery using the voltage and current sensing transducer network and this information is used by the microcontroller to achieve the needed power management control for sustained dc supply to charge the battery. It uses a DC to DC converter circuit to control the dc power from the solar power source to balance the instabilities in solar power. The dc to dc converter circuit uses the SEPIC topology with a pulse-width modulator circuit to achieve control of the dc level of the battery being charged.

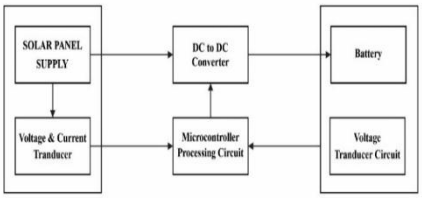

Figure 2: Functional block of the solar pulse-width modulator charger

The system design analysis is presented under the following sub-sections;

2.1 Power Source (Solar Panel)

The solar charge controller helps to control regulated DC power to charge the battery. The DC power source is from a solar panel. The maximum power supply voltage from the solar panels is aimed at 32.3V based on the solar panel rating. The solar panel acquired is a 270W solar panel and its specifications are listed thus;

Maximum Power rating, P_{max} =270W
Voltage at max. power, V_{max} = 32.3V
Current at max. power, I_{max} = 8.36A
Short Circuit current, I_{sc} = 9.06 A
Open circuit Voltage, V_{oc} = 37.8 V
Cell Technology = Monocrystaline

The DC to DC converter would step down the solar voltage to 13.5V for the charge controller.

2.2.1 Design of Power Supply Circuit

The power supply for the control circuit is from the solar panel. The circuit diagram is shown in Figure 3.
The circuit supply needs a power supply of +5V. The circuit consists of an IC voltage regulator, 7805.

The current limiting resistor R_L is to limit current to the voltage regulator.

$$R_L = \frac{V_{sol} - V_{reg}}{I_{reg}} \quad (1)$$

Where,
V_{sol} = solar voltage = 32.3V
V_{reg} = regulator minimum input voltage = 7V
I_{reg} = regulator current = 1A

$R_L = \frac{32.3 - 7}{1} = 31.3\Omega$

The closest value is 10Ω and this was used instead.
Capacitor C1 is optional but added to filter off circuit noise and the chosen values is 10µF.

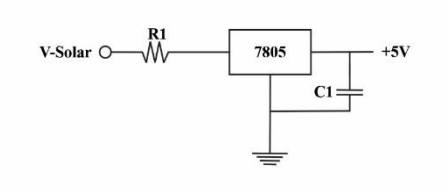

Figure 3: Power Supply circuit

The IC voltage regulator used is the 7805 positive 5V voltage regulator.

7805 Voltage Regulator data;

Maximum input voltage	= 35V
Output voltage	= 5V
Drop out voltage	= 2V
Minimum input voltage	= 7V
Output current	= 1A

2.2.2 Design of the Voltage and Current Sensing Circuit

The sensing circuit functions to bring down the high analog voltage and current to a low value compatible with the microcontrollers onboard analog to digital converter (ADC) which is 2V maximum.

A voltage divider was used for dc voltage sensing and level measurement while a series resistor was used as the current sensor.

Figure 4. shows the current sensing resistor and a voltage divider. The same was applied for solar and the battery voltage reading;

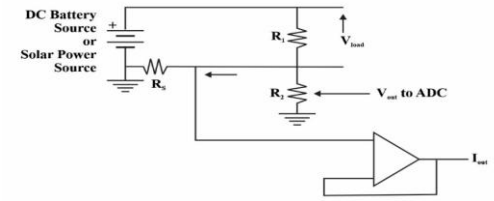

Figure 4: Circuit Diagram of the Voltage and current sensing Circuit

According to ohm's law the voltage developed across R_s is directly proportional to the load current.

$V_s = I_L R_s$ (2)

Where;

V_s = sensor voltage

I_L = load current

R_s = sensor resistance

For a sensor load voltage of 1V from R_s with load current of 10A

$$R_s = \frac{1.0}{10} = 0.1\Omega = 100\text{m}\Omega$$

R_1 and R_2 form the voltage divider circuit for voltage level sensing.

R_2 was chosen to be a variable resistor for fine-tuning and calibration purposes.

For a current flow assumed to be 1.0mA flowing through R_1 and R_2 in series and for a maximum solar voltage of 32.3V, then total resistance is:

$$R_T = \frac{V_{sol}}{I_t} \quad (3)$$

Where R_T is the total resistance of the voltage divider of R_1 and R_2 and I_t is the current through them.

I_t = 1.0mA (chosen)

$$R_T = \frac{32.3}{1.0 \text{ X } 10^{-3}} = 32.3\text{k}\Omega$$

This value was shared between both resistors. A value of 10kΩ variable resistor was used for R_2 and R_1 was 10kΩ.
From the voltage divider expression,

$$V_{out} = V_{in}\left[\frac{R_2}{(R_1 + R_2)}\right] = 32.3\left[\frac{10\,000}{(10\,000 + 10\,000)}\right] = 16.15V \quad (4)$$

The operational amplifier was used as a voltage follower for its impedance matching properties to interface the current that was converted to a voltage by R_s to the ADC input.
The dual op-amp LM358 was used for all the operational amplifier voltage follower circuitry because of the economy and good slew rate and its unipolar operational ability. Figure 5 shows the pin assignment of the op-amp.

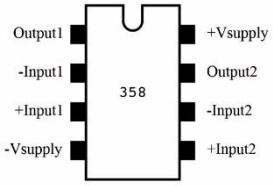

Figure 5: Pin layout of the LM358 dual Op-Amp

2.2.3 PIC16F88 Microcontroller Circuit

The microcontroller used for this work is the microchip PIC16F88 model. It was chosen for this work because of its large EEPROM memory capacity and its onboard analog to digital converter (ADC) and RS232 serial engine.

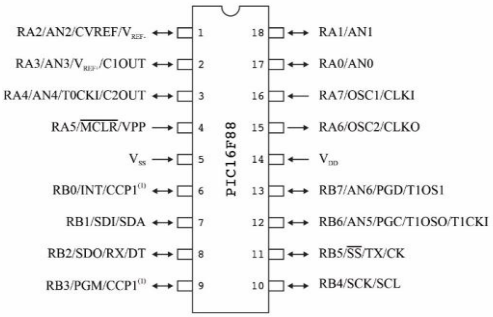

Figure 6: Pin layout of the PIC16F88 Microcontroller
NOTE: The CCP1 pin is determined by the CCPMX bit in Configuration Word 1 register

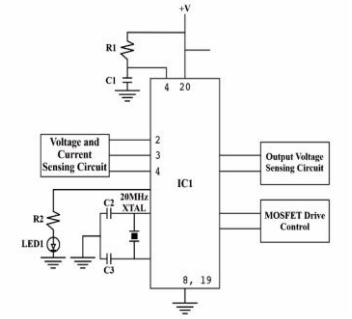

Figure 7: Microcontroller circuit
Figure 7 shows the microcontroller circuit and its accompanying components.
Pin 15 and16 are for the oscillator. The oscillator of choice for the microcontroller (IC1) is the 4 MHz crystal oscillator for high-speed operation which is programmed from the codes because the design needs precise control of timing in its control processes.
Pin 4 is the master clear terminal and it was used to achieve external start-up delay for the microcontroller.
R1 and C1 determine how long the microcontroller will remain in the reset state until power surge subsides before it will start working. This is necessary so that the microcontroller internal clock will not be affected by power supply surge transients when powered for the first time.

The microcontroller uses a 4 MHz crystal for the internal oscillator and this will result in the instruction cycle value as;
Oscillator frequency F = 4 000 000 Hz

Period, $T = \frac{1}{F} = \frac{1}{4\,000\,000} = 0.25\mu s$

Clock frequency, $F_C = \frac{\text{Oscillator Frequency}}{4} = \frac{4\,000\,000}{4} = 1\,000\,000$ Hz (5)

Instruction cycle, $T_s = \frac{1}{F_c} = \frac{1}{1\,000\,000} = 1\ \mu s$ (6)

Let the start-up delay time $T_s = 0.7R_1C_1$
For a time $T_s = 40\ \mu s$ and $C_1 = 10$ nF, thus

$R_1 = \frac{T_s}{0.7C_1} = \frac{40 \times 10-6}{0.7 \times 10 \times 10^{-9}} = 5.6\ k\Omega$

The microcontroller has 10bits, 5 channels ADC inputs. One of the inputs (pin 5) was used as the reference pin for the ADC leaving 4 ADCs for use. The design requires the measurement of parameters such as the battery voltage, solar voltage, and solar current.
The red LED used indicates when the circuit is active while the green LED indicates battery charging and full charge. The LEDs have a voltage drop of 2.2V at 8mA.
Hence limiting resistance would be:

$R_2 = \frac{V_{cont} - V_d}{I_d} = \frac{5 - 2.2}{8 \times 10^{-3}} = 350\Omega$ (7)

where V_{cont} = controller output voltage of 5V, a value of 330Ω was chosen as closest standard

2.2.4 DC to DC Converter

The dc to dc converter stage was used to convert the solar voltage from one level to another. For this design, it is expected to convert the 32.3V dc voltage from the solar panel to 13.5V dc to charge the battery. The use of it is due to the function of impedance matching improvement it offers for maximum power transfer of energy from the solar panel to the load.

The dc to dc converter uses the single-ended primary inductance converter (SEPIC) topology. The SEPIC topology was used because it has a single switch driver to achieve buck and boost functions simply through pulse width adjustment which means it provides a positive regulated output voltage from the solar panel voltage that varies from above to below the output voltage.
The dc to dc converter circuit used in this design consists of two stages namely;
SEPIC converter
Pulse Width Modulator Driver

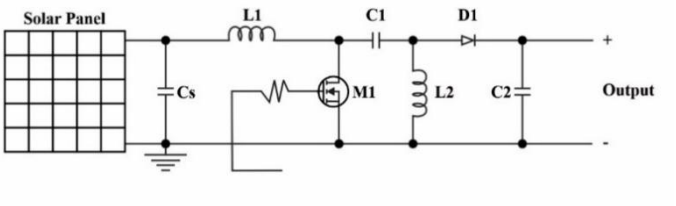

Figure 8: Circuit diagram of the SEPIC Converter

2.2.5 SEPIC Converter

The SEPIC converter has the following specifications that would serve as the basis for getting the values for the components.
Input voltage or source voltage $V_{IN(MAX)} = V_S = 32.3V$
$V_{IN(MIN)} = 15V$
Output / load voltage $V_O = 13.5V$
Output current, $I_o = 10A$
Power, $P = V_o \times I_o = 13.5 \times 10 = 135W$
Worst case efficiency = 90% = 0.9
Operating frequency, F = 20 kHz

Maximum Duty ratio, $D = \frac{V_O + V_{FWD}}{V_{IN(MIN)} + V_O + V_{FWD}} = \frac{13.5+1}{15+13.5+1} = 0.49$ (8)

Where V_{FWD} = Forward Voltage Drop of diode = 1V

$D_{(MAX)} \approx 0.5 = 50\%$

Solving the average inductor current through L_1 which is also the average source current;

$I_{L1(MAX)} = I_S = \frac{I_O V_O}{V_{IN(MIN)} \times \eta} = \frac{13.5 \times 10}{15 \times 0.9} = 10A$ (9)

Where η = efficiency

Output current for output of 13.5V,

$I_O = 10A$

The inductor sizes are chosen such that the change in inductor current is no more than 10 % of the average inductor current. A rule of thumb is to pick between 20% to 40%. A value of 30% was chosen for this design.

Thus, $\Delta i_{L1} = 0.3 \times I_{L1} = 0.3 \times 10$

$\Delta i_{L1} = 3A$

The change in inductor current expression is;

$\Delta i_{L1} = \frac{V_S D}{L_1 F}$ (10)

This ripple change would require inductor size of;

$L_1 = \frac{V_S D}{F \Delta i L_1} = \frac{15 \times 0.5}{20\,000 \times 3} = 125\ \mu H$ (11)

Solving for L_2 with the 30% ripple in inductor current, then

$\Delta i_{L2} = \frac{V_S D}{L_2 F}$ (12)

$\Delta i_{L2} = 0.3 \times I_O = 0.3 \times 10 = 3A$

$L_2 = \frac{V_S D}{F \Delta i L_2} = \frac{13.5 \times 0.5}{20\,000 \times 3} = 112.5\mu H$ (13)

The variation is expected to be between 13V to 14V and this will result in the following;

Output voltage variation $\Delta V_O = 14 - 13 = 1V$

The change in output voltage which is also the output ripple voltage is also the ripple voltage across capacitor C_2

$\Delta V_O = \Delta V_{C2} = \frac{V_O D}{R C_2 F} = 1V$

Solving C_2

$C_2 = \frac{D}{R\left(\frac{\Delta V_O}{V_O}\right)}$ (14)

Replacing $R = \frac{V_O}{I_O}$

$C_2 = \frac{D}{\left(\frac{\Delta V_O}{I_O}\right) F} = \frac{0.5}{\left(\frac{1}{10}\right) \times 20\,000} = 250\ \mu F$ (15)

A value of 250 µF was used.

Solving for capacitor C_1

$C_1 = \frac{D}{R\left(\frac{\Delta V_{C1}}{V_O}\right)}$ (16)

Replacing $R = \frac{V_O}{I_O}$

$C_1 = \frac{D}{\left(\frac{\Delta V_{C1}}{I_O}\right) F}$ (17)

Variation allowed for C_1 is,

$\Delta V_{C1} = V_{IN(MAX)} - V_{IN(MIN)}$ (18)

Where

$V_{IN(MAX)}$ = maximum input voltage = 32.3V and

$V_{IN(MIN)}$ = minimum solar voltage to maintain output

$V_{IN(MIN)} = V_{out}$ + drop across element like diode and inductor (19)

$\Delta V_{C1} = 19 - (13.5 + 1) = 4.5$

$C_1 = \frac{0.5}{\left(\frac{4.5}{10}\right) \times 20\,000} = 56\ \mu F$

2.3 Design of Pulse Width Modulator

The microcontroller served as the pulse width modulator stage and so generates the pulses to drive the MOSFET in the SEPIC converter.

The MOSFET stage is the switch for the SEPIC converter.

The peak current the MOSFET will conduct during operation is,

$I_{QPK} = I_{IN} + I_O + \Delta I_{L1}$ (20)

$I_{QPK} = 10 + 10 + 3 = 23A$

Root Mean Square current (RMS) I_{QRMS}

$I_{QRMS} = \frac{I_{IN}}{\sqrt{D}}$ (21)

$I_{QRMS} = \frac{10}{\sqrt{0.5}} = 14.14A$

The MOSFET used in the design is the IRFP 260N-channel as it is capable of handling the current for charging.

A fixed resistor of 10kΩ was connected between the gate and source to aid fast switching by discharging any residual static charge at the gate.

2.4 Microcontroller Program and Algorithm

The program code for the microcontroller was developed using assembly language. The software for assembly language is the MPASM of MPLAB 7.40. The codes were compiled by this compiler and downloaded to the PIC16F88 using WINPIC 800 downloader software.

Figure 9 shows the flowchart of the program. The microcontroller uses its onboard analog to digital converter to get the values of the solar voltage and current and the battery voltage. It uses this information to control the pulse width of the pulses generated.

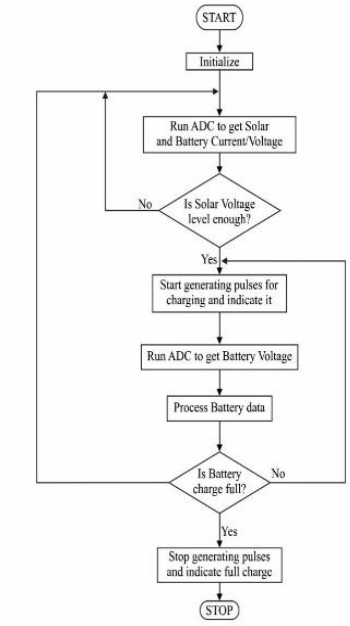

Figure 9: Flowchart for the program for the Microcontroller on the Solar PWM Charger

2.5 Operational Principle of the Solar Charge Controller System

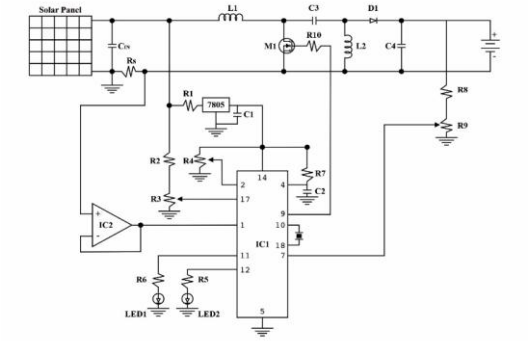

Figure 10 Complete circuit diagram of the Solar PWM Charger

The complete circuit diagram of the solar charge regulator is shown in Figure 10. The circuit shows the circuit components and interconnections.
The circuit is powered by the solar panel.
The power supply stage consists of the IC voltage regulator 7805 whose function is to regulate the 32.3V from the solar panel to 5V to power the circuit.
Resistor R1 is a current limiting resistor to the voltage regulator 7805.
Capacitor C1 filters off any noise voltages that are due to circuit operation and any residual ripple from the supply.
The microcontroller IC1 is the main control device. It monitors the solar voltage level through the voltage divider made up of R2 and R3. It also checks the battery voltage through R8 and R9 and monitors the load current through the R_s current sense resistor.
R_s converts the DC load current to the voltage which is fed to a voltage follower IC1 for impedance matching.
When monitoring the solar voltage, if the solar voltage is above 15V it would start generating pulses for the SEPIC stage to be active. This would cause the battery to charge up and would indicate charging with LED1. When the battery charge is up to 13.5V it would stop charging the battery by stopping the pulse generation.
LED1 is used for battery charging status while LED2 indicates a full charge. Resistors R5, R6 are current limiting resistors to the LEDs 1 and 2.
The solar regulator uses the SEPIC dc to dc converter to regulate the power from the solar to the load. The SEPIC converter is made up of L1, L2, C3, C4 and D1 and the MOSFET switch M1.
The microcontroller IC1 also serves as the pulse-width modulator that drives the MOSFET M1 to keep the SEPIC active and its function is to generate the 20kHz pulses needed to drive the MOSFET. It adjusts the pulse width of the pulses as the battery charge increases. The pulses are narrower as the battery attains full charge level and wider when it is far off it.

2.6 Construction

This section carefully explains the construction process employed in the design of the charge controller. The construction of the circuit was embarked on after the design and acquisition of necessary components from the market and all necessary working tools. The construction sequence is as follows:

i. Inductor/SEPIC Construction
ii. Bread-boarding of Components
iii. Soldering of Circuit Components
iv. Computer Interfacing
v. Test and Results
vi. Casing

2.6.1 SEPIC/Inductor Construction

The inductors were designed with copper wire and ferrite core and the coils were wounded to get the required inductance for L1 and L2. As required, the inductors were wounded by the design with proper care using high-frequency winding technique for reduced losses so it will conform to specification. The ferrite core unit used was brought out from a bad

monitor board as it had the required dimensions needed for the work. It was put apart and the former coils were removed and the new one as specified in the design was wounded into the insulation called the bobbin. With the help of components like a pair of ferrite cores comprising of both "E" sections, a pair of end clamp frame together with the insulated conductors, and a bobbin, the inductors were constructed to the designed specifications with its entire designed taps brought out for external connections.

At the completion of the winding, the bobbin was stacked with the high-frequency transformer core which was a solid ferrite "E"-"E", lamination type and insulation tape was used to hold them in place.

2.6.2 Pre-Testing of Circuit

The pre-testing of the working circuit was done on a breadboard. The circuit was temporarily set up on the breadboard and the test was carried out on the circuit. This pre-test is necessary so that stages that would not respond well can be corrected before the final circuit soldering. The test was carried out after the microcontroller was programmed with the necessary codes.

2.6.3 Soldering of Circuit Components

The permanent soldering of the circuit components on the veroboard was done after the completion of the circuit test on the breadboard with all necessary adjustments effected. Tools/materials such as the soldering iron, lead, lead sucker, copper stripping knife, wire cutter/stripper, long-nose pliers, were used in soldering the component on the veroboard according to the circuit diagrams. The multi-meter helped to check for various connections continuity and discontinuity problems respectively.

2.6.4 Microcontroller Program

Assembly language (MPASM of MPLAB 7.40) was the program code used for the microcontroller. The codes were compiled by this compiler and downloaded to the microcontroller (PIC16F88) using WINPIC800 downloader software.

2.7 Casing

On appropriate consideration of the size of the circuit components, a white plastic panel casing was used as the casing for the work with 10cm x 12cm x 8cm dimensions. Perforation was necessarily made on different sides of the casing to allow for component cooling. Special provisions for input terminals and battery terminals were also carefully made. Space was provided for the various indicators, the active circuit red LED indicator and the full charge green LED indicator separately.

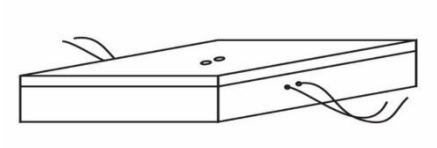

Figure 11: Casing (10cm x 12cm x 8cm dimensions)

3.0 Tests

Figure 12: Test set-up of the charge controller circuit

The test carried out after completion of the soldering of the circuit stages was to first of all check for the power supply voltages and voltages at different nodes in the circuit to see if they are as expected.

As shown in Figures 12 and 13, the final test of the circuit. The solar panel and the 12v 100AH battery were connected to the charge controller circuit. The solar panel as the power source and the battery as the load for charging. The ammeter and voltmeter were connected to the connector of the uncased charge controller circuit, the battery and the solar panel as shown in the schematic diagram in Figure 13

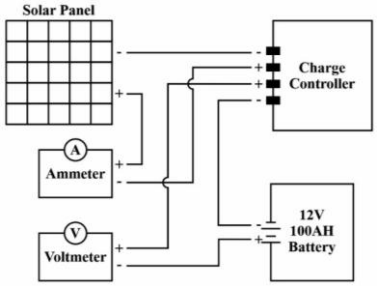

Figure 13: Schematic diagram showing test connections of the Solar Panel, Charge Controller and Battery to the Voltmeter and Ammeter for test readings.

The solar charging voltage and current were monitored at different times as the test was ongoing. Results obtained at 20 minutes time interval on the ammeter and voltmeter respectively, were recorded.

3.1 Results

A discharged battery was gotten to carry out the test.

The battery has the following parameters:

Brand Name: SOLITE
Type Number: Type V2360A
Battery Rating: 12V, 60 AmpHr
Initial Terminal Voltage: 11.1V

The test was achieved by recording the amount of charging current at every twenty (20) minutes interval with the help of the ammeter and voltmeter. A set of readings was taken and recorded as shown in the table below.

Table 1: Results obtained from the operation of the Solar PWM

S/N	Solar Panel		Battery		Remarks	Time (Mins)
	Input Voltage (V)	Input Current (I)	Output Voltage (V)	Output Current (I)		
1.	31.0	0.71	14.2	1.51	Cloudy	11:00
2.	32.1	0.98	14.2	2.23	Sunny	11:20
3.	30.9	0.80	13.9	1.77	Cloudy	11:40
4.	33.9	0.95	14.0	2.25	Sunny	12:00
5.	33.2	1.02	14.1	2.39	Sunny	12:20
6.	29.4	1.38	14.2	2.89	Sunny	12:40
7.	33.0	1.09	14.1	2.56	Sunny	01:00

The table 1 shows that the battery reached a good charge level for just two (2) hours which indicates the system worked as expected. The battery used attained full charge after three hours of rich sunlight on a sunny day.

3.2 Graph / Deductions

3.2.1 Solar Panel Test Deduction

Solar panel input voltage read and solar panel input current measurement is shown in figure 14.

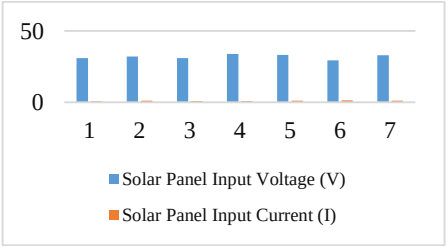

Figure 14: Graph of Solar panel Input Current and Solar panel Input Voltage

From figure 14, it is shown that the average input voltage is 31.9V which is slightly less than the solar panel rated input voltage of 32.3V and at noon, the cloud being bright and sunny, the highest voltage of 33.9V on the voltmeter reading was reached. Also, at 11:00 am, the input current shows the lowest value of 0.71A as a result of the atmosphere being damp. The highest input current of 1.38A at 12:40 pm is reached as a result of intense penetration of light on the solar panel being that the cloud was sunny. The highest input power of 40.572W was reached at 12:20 pm

3.2.2 Battery Test Deduction

Battery output voltage read and battery output input current measurement is shown in figure 15.

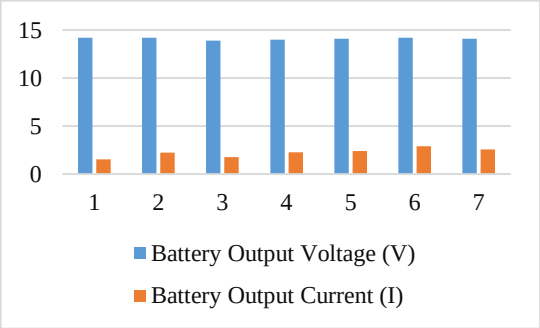

Figure 15: Graph of Battery Output Current and Battery Output Voltage

From figure 15, The average output voltage is 14.1V, 0.4V less than the battery rating of 14.5V, at 11:00 am, the atmosphere being damp, the reading shows the point of a low output current of 1.51A and at 12:40 pm, there was intense light, the atmosphere was sunny, the highest output current of 2.89A was recorded. With high current and high voltage at this point, the battery charged faster.

It should be noted that the point of little or no ammeter reading is points of partial shading on the solar panel. Therefore, the more open the solar panel is to light, the higher the voltage and current which in turn brings about the fast charge of the battery. And also, the less open the solar panel is to light, the lower the voltage and current which in turn brings about slower charge of the battery.

4.0 Conclusion

This study which details the design and construction of a charge controller circuit using Pulse Width Modulation (PWM) was designed, constructed, and tested to evaluate its performance. At completion, it was able to charge a 12V battery successfully.

The principles employed in realizing the solar PWM charge controller circuit were highlighted and explained, including presentation of the design calculations, and procedures carried out while designing, constructing, and testing of the circuit.

Quite a few difficulties were encountered during the testing stage, one of which involved adjusting component values to get good pulse width variation to change the charging voltage of the battery as it progresses towards full charge. These difficulties were in due course overcome.

It is recommended that a better pulse width modulation algorithm be developed to work with the microcontroller towards achieving tighter control of the pulse width variation to the load. It is also recommended that the use of maximum power point tracking technique combined with pulse width modulation be explored for its use in designing a more efficient battery charging system.

REFERENCES

[1] https://pediaa.com/difference-between-primary-and-secondary-cells/
[2] https://physicsmax.com/primary-secondary-cells-7647
[3] https://cycledoctor.com/battery-tutorial/
[4] https://www.instructables.com/id/Best-Sealed-Lead-Acid-Battery-Recovery/
[5] https://www.scribd.com/document/300832113/Parameter-Identification-of-the-Lead-Acid-Battery-Model
[6] https://www.usgbc.org/articles/top-four-benefits-installing-solar-panels-your-home